

# We are IntechOpen, the world's leading publisher of Open Access books Built by scientists, for scientists

4,800

Open access books available

122,000

International authors and editors

135M

Downloads

Our authors are among the

154

Countries delivered to

TOP 1%

most cited scientists

12.2%

Contributors from top 500 universities



WEB OF SCIENCE™

Selection of our books indexed in the Book Citation Index  
in Web of Science™ Core Collection (BKCI)

Interested in publishing with us?  
Contact [book.department@intechopen.com](mailto:book.department@intechopen.com)

Numbers displayed above are based on latest data collected.  
For more information visit [www.intechopen.com](http://www.intechopen.com)



---

## A Combined Molecular Docking and Electronic Structure Study for a Breast Cancer Drug Design

---

Linda-Lucila Landeros-Martinez,  
Daniel Glossman-Mitnik,  
Erasmus Orrantia-Borunda and  
Norma Flores-Holguin

Additional information is available at the end of the chapter

<http://dx.doi.org/10.5772/intechopen.72895>

---

### Abstract

The molecular docking of tamoxifen's metabolites, 4-hydroxy-tamoxifen, N-desmethyl-tamoxifen, and 4-hydroxy-N-desmethyl-tamoxifen, in estrogen and progesterone hormone receptors was studied in aqueous solution. The metabolites 4-hydroxy-tamoxifen, N-desmethyl-tamoxifen, and 4-hydroxy-N-desmethyl-tamoxifen exhibit a binding energy in the estrogen receptor cavity of  $-10.69$  kcal/mol,  $-10.9$  kcal/mol, and  $-11.35$  kcal/mol, respectively, and  $-1.45$  kcal/mol,  $-9.29$  kcal/mol, and  $-0.38$  kcal/mol in the progesterone receptor. This indicates a spontaneous interaction between the metabolites and the active sites in the hormone receptors. Docking has an adequate accuracy for both receptors, and from this calculation the active site residues were defined for the different metabolites and the estrogen and progesterone receptors. Also, the chemical reactivity of the amino acids of the active sites of each metabolite was determined. These reactivity properties were obtained within the framework of density functional theory, using the functional M06 with the basis set 6-31G (d). The results indicate that in the estrogen receptor, the highest charge transfer of the three analyzed metabolites is in the union of the metabolite and the Leu346-Thr347 residue. The progesterone receptor shows minor tendency to react with higher hardness values than the estrogen receptor. The hydrogen bonds are three for the estrogen receptor in two different metabolites, while in progesterone only one is formed with the N-desmethyl-tamoxifen metabolite.

**Keywords:** molecular docking, tamoxifen, binding energy, charge transfer, hydrogen bond, hormone receptors

---

## 1. Introduction

Breast cancer is the leading cause of cancer death in women. A prognosis of breast cancer can be issued because there are parameters that predict the evolution or aggressiveness of the cancer, such as lymph nodes, tumor size, and histological grade of cancer [1–4]. In mammary cells there are hormone receptors (estrogen receptors (ERs) and progesterone receptors (PRs)) that function as “switches,” activating or deactivating a particular function in the mammary cell.

Over the last two years a number of drugs have been developed with specific properties for the treatment of breast cancer. Fulvestrant is a steroid-based selective estrogen receptor downregulator (SERD) that antagonizes and degrades ER- $\alpha$  and is active in patients who have progressed to antihormonal agents [5]. Also, the selective ER modulators (SERMs)/SERD hybrids (SSHs) have been used to facilitate the first-line treatment for ER 1 degradation in breast cancer cells [6].

Another important piece of research by Srinivasan et al. presents the discovery of a series of SERDs lacking a prototypical side chain. This absence improves the mechanism called “indirect antagonism” [7]. The latest developments have found the optimal design of antiestrogen cores and side chains with the middle structures of the original SERMs class, such as tamoxifen (TAM), raloxifene, lasofoxifene, and bazedoxifene. Also, current studies of SERDs have been made by GlaxoSmithKline(GSK), Genentech, and AstraZeneca. In these studies the side chain is modified to a simple adamantyl core [8].

In addition, for several years, have been used antibodies as cancer drugs, and some examples are trastuzumab and pertuzumab, which are used in breast cancer as the only component. In fact, efforts have been made to use the antibodies conjugated with a variety of substances with the aim of improving their effect. Research on cancer therapy is still in progress [9].

TAM is a SERM [10, 11] and is used for the treatment of hormone receptors expressing breast cancer [12]. This drug is metabolized in the liver, producing three different metabolites: 4-hydroxy-tamoxifen (4OHTAM), N-desmethyl-tamoxifen (NDTAM), and 4-hydroxy-N-desmethyl-tamoxifen, also known as endoxifen (END) [13, 14]. These metabolites show a range of agonist and partial antagonist activities of ER-mediated effects [15]. In vivo studies have shown that TAM competes against estrogens to dock to the receptors, resulting in an attenuation of the cellular response measured by estrogen [16]. Therefore, the clinical response to TAM therapy will depend on the total effect of the resulting metabolites on the patient, their affinity for receptors, and their agonist/antagonist profile [15].

Recently, a number of theoretical studies on TAM and some of its active metabolites have described its interaction with ERs. Calculations of molecular dynamics have been used to model dynamic fluctuations in structures of ERs (ER- $\alpha$  following the binding to estradiol and the metabolite 4OHTAM) [17]. Recently, in an article written by the authors, the molecular docking of TAM in ER and PR was presented in which the active site of the hormone receptors was determined, as well as the charge transfer of the drug to the amino acids of the active sites of the receptors [18]. Other theoretical studies analyzed the chirality of TAM using density

functional theory (DFT) with functional B3LYP and BLYP with a basis set 6-311++G(2d, 2p) [12]. In addition, there was a reported analysis of the amount of charge transfer and the direction of the flow of charge of alkylating drugs in the presence of DNA bases allowing prediction among its bases of which one is the main target of these antitumor drugs [19].

Another technique is molecular docking, which is a computational procedure that attempts to predict noncovalent binding of macromolecules (receptor) and small molecules (ligands) efficiently [20]. In detail, docking consists of an operation in which one molecule is brought into the vicinity of another while calculating the interaction energies of the many mutual orientations and conformations of the two interacting species. A docking procedure is used as a guide to identify the preferred orientation of one molecule relative to the other [21]. This method plays a key role in promoting fundamental biomolecular events such as enzyme–substrate, drug–protein, and drug–nucleic acid interactions [22]; it is also widely used in drug design [23]. Some authors have used the molecular docking of macromolecules to define the energy and bonding affinity in ER- $\alpha$  and ER- $\beta$  with estrogen [24]. It has also been used in the analysis of a maltogenic amylase of *Bacillus lehensis* G1, which provides a view of the substrate and specificity in the macromolecule [25], and in the DNA docking analysis of natural products such as methyltransferase inhibitors, which have become an alternative for cancer therapies [26].

The objective of this research is to develop molecular docking of the metabolites of TAM with the macromolecules ER and PR, to obtain an active site of the hormone receptors. To perform computational protein–ligand docking experiments, a 3-D structure of the target protein at atomic resolution must be available. The most reliable sources are crystal and solution structures provided by the Protein Data Bank (PDB) [26, 27]. The hormone receptors selected for this work are the 1A52 ER- $\alpha$  ligand-binding domain complexed to estradiol, and the 1A28 hormone-bound human progesterone receptor ligand-binding domain. Both belong to the organism *Homo sapiens* and are present in breast cancer cells. Molecular docking has the advantage of working on a large scale, as well as determining the important sites of the macromolecule (active sites) [27, 28]. Once the active site is defined, an accurate calculation of electronic structure can be developed with methods such as DFT, which is the most popular, efficient, and versatile tool for obtaining precise information of molecular systems. For both receptors, the amino acids (residues) forming the active site were analyzed in an attempt to obtain their electronic properties such as ionization potential, electron affinity, electrophilicity, chemical hardness, chemical potential, and electronegativity. A transfer and charge flow direction analysis was also performed.

## 2. Computational details

### 2.1. Molecular docking

Molecular docking is calculated with the specially tailored software AutoDock 4.2 with the Lamarckian Genetic Algorithm (LGA) [28, 29] to explore how ER and PR bond with the metabolites. AutoDock uses a semiempirical free energy force field to predict binding free energies of

small molecules to macromolecule targets [29]. The force field is based on a comprehensive thermodynamic model that allows incorporation of intramolecular energies into the predicted free energy of binding. It also incorporates a charge-based method for evaluation of desolvation designed to use a typical set of atom types [30]. The use of LGA allows individual conformations to search their local conformational space, find local minima, and then pass this information to later generations [29]; also LGA can handle ligands with more degrees of freedom and is efficient, reliable, and successful [31].

The water molecules in the receptors are eliminated and only the polar H atoms are added. The docking area is selected by constructing a grid box, size  $52 \times 36 \times 34$  points, centered at x, y, and z coordinates of 89.304, 14.745, and 70.512, respectively, for ER, and a grid box, size  $20 \times 18 \times 26$  points, centered at x, y, and z coordinates of 36.999, 31.767, and 42.694, respectively, for PR using in both receptors a grid spacing of 0.375 Å in AutoGrid [28, 29]. The docking parameters used for the LGA-based conformational searches are: docking trials—150; population size—150; maximum number of energy evaluations—25,000,000; maximum number of top individuals to survive to next generation—1; rate of gene mutation—0.02; rate of crossover—0.8; mean of Cauchy distribution for gene mutation—0.0; variance of Cauchy distribution for gene mutation—1.0; and number of generations for picking the worst individual—10.

## 2.2. Electronic structure calculations

The energy calculations of the amino acids that make up the active site on ER, PR, and TAM metabolites are calculated with the functional hybrid meta-GGA M06 [32, 33] developed by the Truhlar Group from the University of Minnesota, combined with the basis set 6-31G (d) proposed by Pople [34] and the conductor-like polarizable continuum model (CPCM) [35] using water as a solvent. All calculations were made using DFT [35–38] with the Gaussian program 09 [39]. The charge distribution for amino acids and metabolites was obtained with the population analysis of Hirshfeld charges [40].

Equations	
$\eta = \frac{(I - AE)}{2}$	(1)
$\chi = \frac{(I + AE)}{2}$	(2)
$\omega = \frac{\mu^2}{2\eta}$	(3)
$\mu = -\chi$	(4)
$\Delta N = \frac{\mu_B - \mu_A}{2(\eta_A + \eta_B)}$	(5)

**Table 1.** Global reactivity and charge transfer parameters.

The chemical reactivity descriptors of the studied molecular systems were calculated using the DFT conceptual framework. These parameters include ionization potential ( $I$ ), electron affinity ( $EA$ ), chemical hardness ( $\eta$ ) [41], electronegativity ( $\chi$ ) [41], electrophilicity ( $\omega$ ) [42], and chemical potential ( $\mu$ ) [42]. The overall interaction between metabolites and the amino acids that make up the active site on ER and PR can be identified by the charge transfer. This parameter determines the behavior of the different molecular systems as a donor or as an acceptor system. In this case, the electrons transferred from the metabolites to the amino acids of the active site of receptors or vice versa. The global interactions between two constituents can be determined using the charge transfer parameter ( $\Delta N$ ) [43].

The equations of the reactivity and charge transfer descriptors are shown in **Table 1**.

### 3. Results and discussion

#### 3.1. Validation docking

Validation docking was performed for each hormone receptor using the PyMOL program [44]. **Figure 1** shows the structure of the native co-crystallized TAM bond and its metabolites. The root mean square deviation (RMSD) between TAM and the metabolites was calculated for each

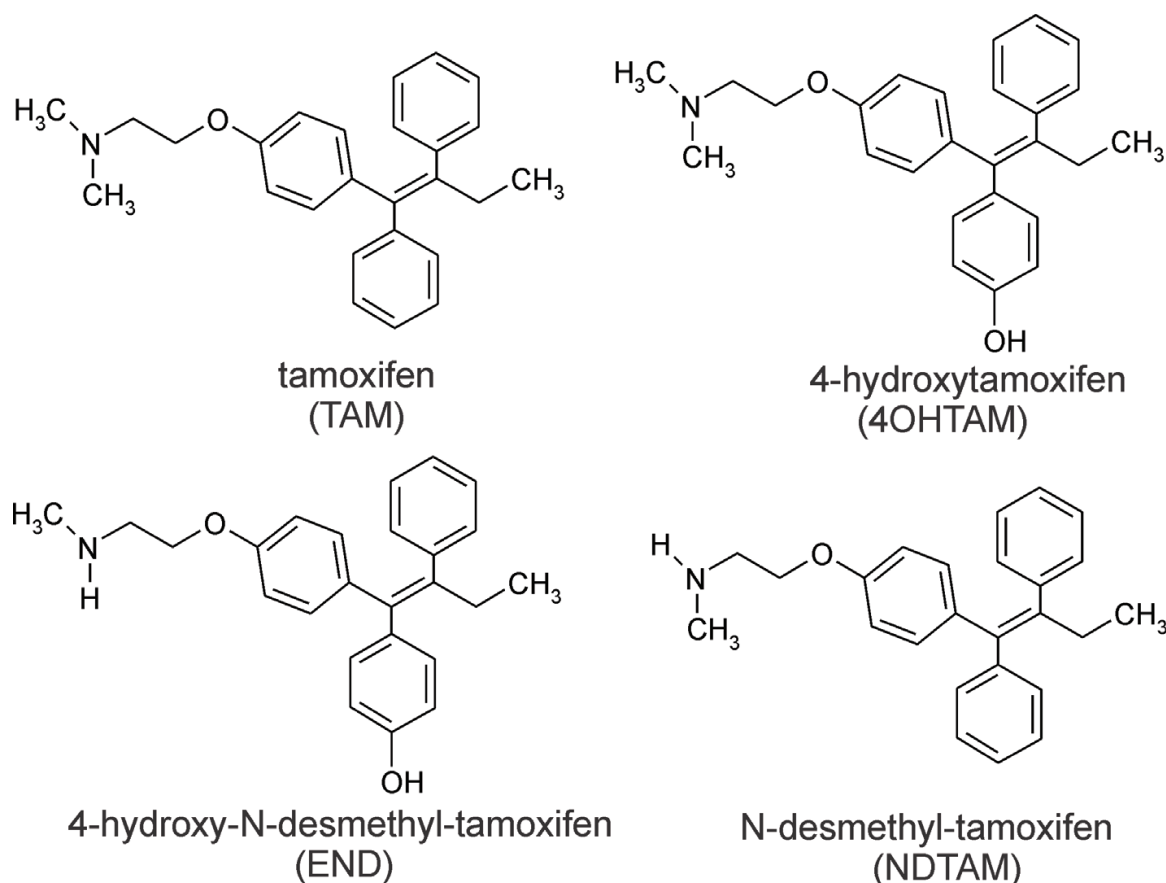


**Figure 1.** Chemical structures of tamoxifen and metabolites.

of the hormone receptor dockings. An RMSD value is considered a measurement of the accuracy of the docking results. The optimal position is recognized if the RMSD value is less than 2 Å [45]. In the case of metabolite dockings, TAM was used as the template for molecular overlap, as it is known that this drug is metabolized into the metabolites analyzed in this study. The metabolites were aligned by rotation and translation to obtain the RMSD using the "Align" option in PyMOL. Therefore, the RMSD in ER obtained between TAM with 4OHTAM, END, and NDTAM is 0.672, 1.106, and 1.461, respectively. For PR the RMSD obtained between TAM and 4OHTAM, END, and NDTAM is 1.387, 2.006, and 0.953, respectively. **Figure 2** shows the alignment between TAM (black) and 4OHTAM, END, and NDTAM (gray).

### 3.2. Analysis of the estrogen receptor with the metabolites

An analysis of molecular docking of the metabolites in ER was carried out, revealing the active site of the ER, followed by its description, the analysis of the chemical reactivity parameters of the residues and the metabolites, as well as the description of the hydrogen bonds between the metabolites and the ER active site.

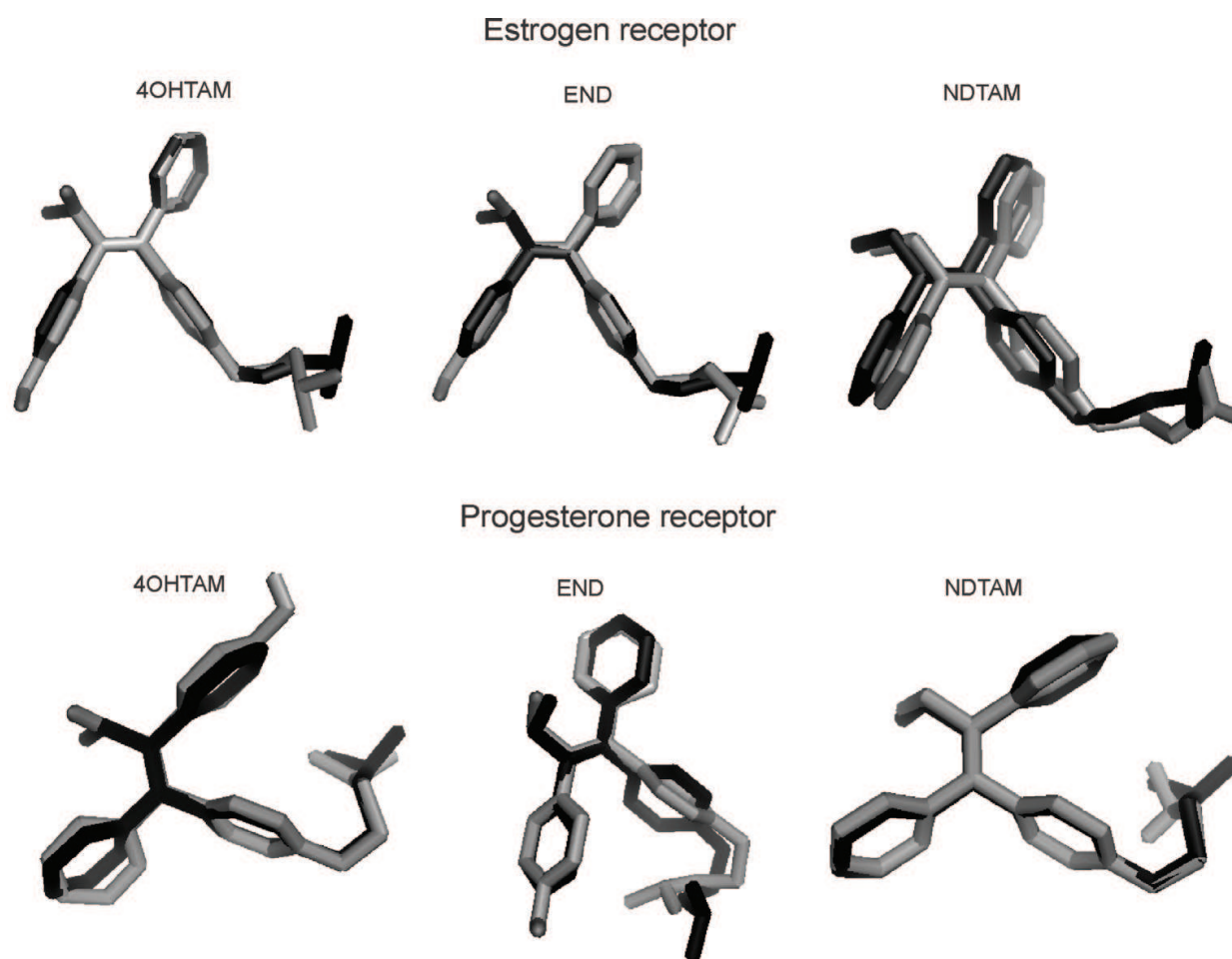


**Figure 2.** Conformation of tamoxifen and metabolites after docking in hormone receptors.

### 3.2.1. Molecular docking

The binding energy of the metabolites with the ER active site was predicted with molecular docking calculations. The negative value of the binding energy (affinity) in the docking indicates that the system is stable and that there is an interaction between ER and the metabolites in the active site:  $-10.69$  kcal/mol for 4OHTAM,  $-11.35$  kcal/mol for END, and  $-10.90$  kcal/mol for NDTAM. It was observed that the binding affinity was lower in 4OHTAM; this is due to the effect of the orientation of the metabolite within the active site caused by the influence of the tertiary amine functional group containing the 4OHTAM.

Finally, the binding energy shows that END, which exhibits  $-11.35$  kcal/mol, is the metabolite with the highest affinity with the active site. It even shows a better affinity than TAM at  $-10.38$  kcal/mol [18]. This coincides with previous information reported by Clarke [46] who says that END has an affinity for ERs higher than NDTAM or TAM itself. As can be observed, all the metabolites have a high affinity to the receptor. According with Gareth [47], the greater the affinity of the ligand for the receptor, the more easily it binds to that receptor. This is important because the binding of a drug to a receptor stimulates the physiological response that characterizes the action of the drug, which means that release of a series of biochemical events results in a biological or pharmacological effect [47].

The schematic structure of the active site and the binding energies are shown in **Figure 3**.

### 3.2.2. Active site

The conformational coupling of the active site with each metabolite is described below.

*4OHTAM*. There are 14 residues in contact with the metabolite 4OHTAM at the active site of the ER. Nine of them are linked forming an amino acids sequence: leucine346-threonine347 (Leu346-Thr347), tryptophan383-leucine384 (Trp383-Leu384), glutamic acid353-leucine354 (Glu353-Leu354), and leucine349-alanine350-aspartic acid351 (Leu349-Ala350-Asp351). The other five are: glycine residue (Gly521)—glycine is the smallest of the amino acids. It is ambivalent, which means that the amino acid can be inside or outside of the protein molecule; lysine529 (Lys529)—this residue contains a protonated amino group that provides a positive charge to proteins as acetyltransferases; histidine524 (His524)—this residue has a positively charged imidazole functional group. This group participates in enzyme-catalyzed reactions; phenylalanine404 (Phe404)—an essential amino acid, it is a derivative of alanine with a phenyl substituent on the  $\beta$  carbon. Due to its hydrophobicity, phenylalanine is nearly always found buried within a protein. The  $\pi$  electrons of the phenyl ring can stack with other aromatic systems and often do so within folded proteins, adding stability to the structure; and finally, methionine388 (Met 388), which has a hydrophobic thiol ether in its lateral chain. According to the results obtained by theoretical calculations, in the metabolite 4OHTAM the active site of estrogen coincides with that reported by Shiau et al. [48].

*END*. The active site of END is formed by the following residues: leucine346-threonine347 (Leu346-Thr347), leucine387-methionine388 (Leu387-Met388), tryptophan383-leucine384 (Trp383-Leu384), glycine521 (Gly521), and histidine524 (His524). The last two residues are highly hydrophilic.



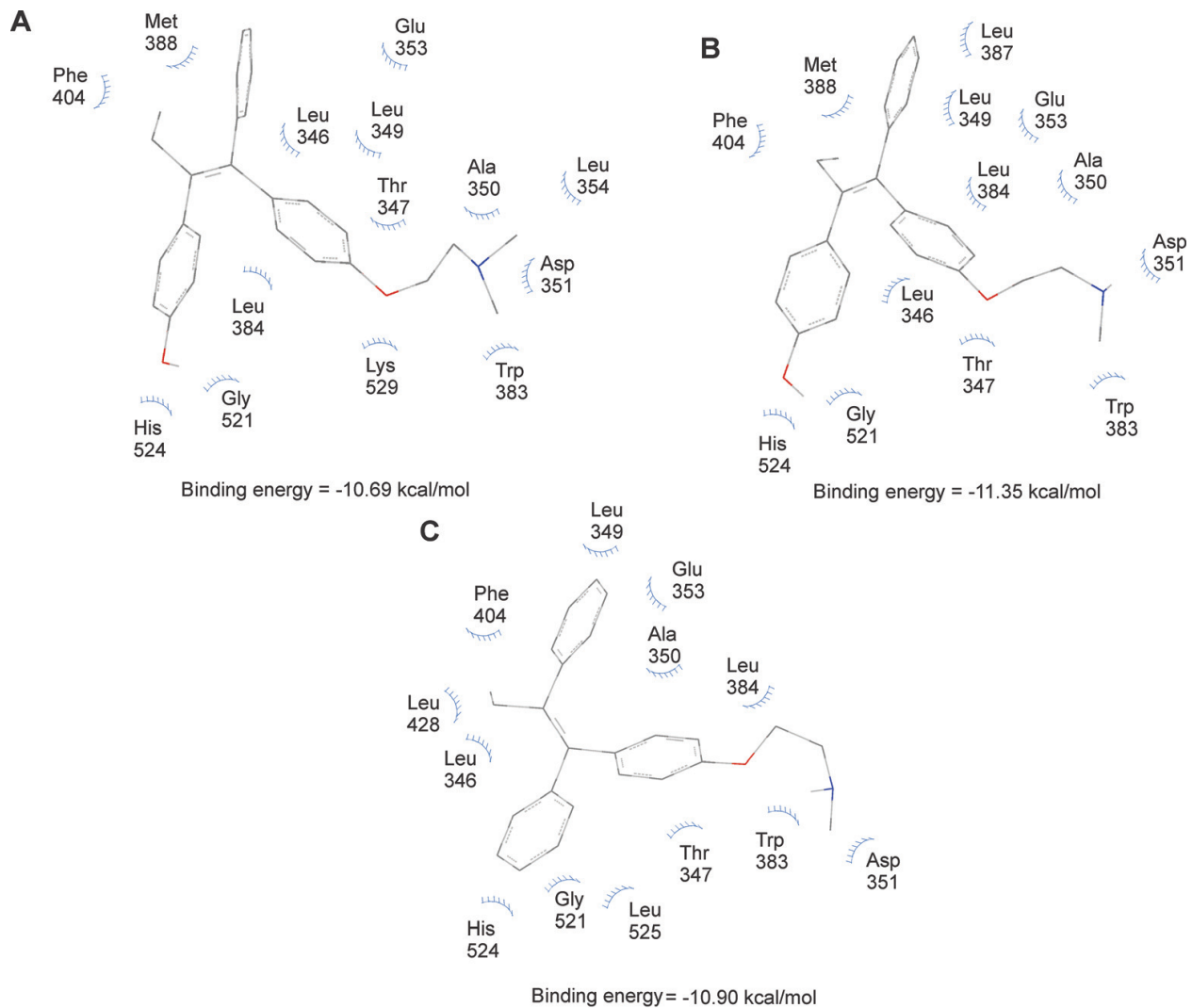


**Figure 3.** Amino acids of the active site of the estrogen receptor with (A) 4OHTAM, (B) END, and (C) NDTAM.

*NDTAM*. The active site in *NDTAM* consists of the following residues: leucine346-threonine347 (Leu346-Thr347), histidine524-leucine525 (His524-Leu525), tryptophan383-leucine384 (Trp383-Leu384), and (Leu349-Ala350-Asp351), and hydrophilic residue glycine521 (Gly521) and hydrophobic residues phenylalanine404 (Phe404), glutamic acid (Glu353), and leucine428 (Leu428).

Most of the residues are situated over the planar core of the ligand. The others surround the functional groups amine and hydroxyl. These interactions contribute to binding energies of up to  $-10$  kcal/mol.

The metabolites act by blocking the activation domain AF-2 of ER found in the ligand bond domain or LBD of the active site. Therefore, the metabolites act as estrogen antagonists over the genes that require only the activation domain AF-2 [49, 50].

The residues for the metabolites in ER are shown in **Figure 3**.

### 3.2.3. Chemical reactivity

Once the most stable structure of the active site of TAM's metabolites were defined, an analysis of the reactivity of ER residues was performed using descriptors such as ionization potential ( $I$ ), electron affinity ( $EA$ ), chemical potential ( $\mu$ ), chemical hardness ( $\eta$ ), and electrophilicity ( $\omega$ ). Calculated results for the reactivity parameters of the drug and residues of the ER are shown in **Table 2**.

The electron affinities of the residues fluctuate from 0.21 eV to 0.91 eV. The highest value of electron affinity is for the Trp383-Leu384 residue, which is present in the active site of the three different metabolites analyzed in this work. According to the ionization potential results, the residue with the greatest possibility of losing electrons is Leu346-Thr347 with 7.74 eV. This residue is present in the active site of the three metabolites.

Metabolite	Active site	EA (eV)	I (eV)	$h\eta$ (eV)	$\mu = -\chi$ (eV)	$\omega$ (eV)
4OHTAM	Gly521	0.21	7.03	3.41	3.62	1.92
	Met388	0.46	6.11	2.82	2.39	1.91
	His524	0.43	6.2	2.89	3.31	1.9
	Lys529	0.83	7.22	3.19	4.02	2.54
	Phe404	0.51	6.4	2.95	3.46	2.03
	Trp383-Leu384	0.91	6.04	2.56	3.47	2.35
	Glu353-Leu354	0.66	5.59	2.47	3.13	1.98
	Leu346-Thr347	0.88	7.74	3.43	4.31	2.71
	Leu349-Ala350-Asp351	0.73	5.79	2.53	3.26	2.1
END	Gly521	0.21	7.03	3.41	3.62	1.92
	His524	0.43	6.2	2.89	3.31	1.9
	Leu387-Met388	0.51	6.25	2.87	3.38	1.99
	Leu346-Thr347	0.88	7.74	3.43	4.31	2.71
	Trp383-Leu384	0.91	5.79	2.53	3.26	2.1
NDTAM	Gly521	0.21	7.03	3.41	3.62	1.92
	Phe404	0.51	6.4	2.95	3.46	2.03
	Glu353	0.2	5.62	2.71	2.91	1.57
	Leu428	0.47	7	3.23	3.73	2.14
	His524-Leu525	0.81	6.1	2.65	3.46	2.25
	Trp383-Leu384	0.91	6.04	2.56	3.47	2.35
	Leu346-Thr347	0.88	7.74	3.43	4.31	2.71
	Leu349-Ala350-Asp351	0.73	5.79	2.53	3.26	2.1

**Table 2.** Parameters of chemical reactivity of the active site residues of the estrogen receptor.

Chemical hardness ranges from 2.53 eV to 3.43 eV; this parameter measures the resistance to change in the electronic configuration. The Glu353-Leu354 residue with 2.47 eV will react more easily in the presence of 4OHTAM, the Leu349-Ala350-Asp351 residue with 2.53 eV will react more easily in the presence of NDTAM, and the Trp383-Leu384 residue with 2.56 eV will react more easily in the presence of END. The chemical potential ( $\mu = -\chi$ ) represents the average effect between the tendency among molecules to attract and transfer electrons. This parameter is an important part in the description of the charge transfer descriptor. The electronegativity shows that the Leu346-Thr347 residue has the greatest tendency to attract electrons with 4.31 eV. This trend is repeated with the three different metabolites. Electrophilicity  $\omega$  represents the stabilization energy of the systems when it becomes saturated with electrons coming from the surroundings. In this case, in the active site of 4OHTAM, value decreases in the following order: Leu346-Thr347 > Lys529 > Trp383-Leu384 > Leu349-Ala350-Asp351 > Phe404 > Glu353-Leu354 > Gly521 > Met388 > His524. In END the decreasing order is Leu346-Thr347 > Trp383-Leu384 > Leu387-Met388 > Gly521 > His524 and in NDTAM the decreasing order is Leu346-Thr347 > Trp383-Leu384 > His524-Leu525 > Leu428 > Leu349-Ala350-Asp351 > Phe404 > Gly521 > Glu353.

#### 3.2.4. Charge transfer descriptor

The chemical reactivity descriptors mentioned above are intramolecular parameters, whose values are calculated from the electronic properties of the molecule. To understand a chemical reaction in depth an intermolecular parameter that represents the fractional number of electrons transferred from one system to another should also be considered. This parameter is called charge transfer and is described as Eq. 5 in **Table 1**. In this formula,  $\mu_A$  is TAM's metabolites and  $\mu_B$  is the chemical potential for the residues of the active site.  $\eta_A$ ,  $\eta_B$  represent the chemical hardness of TAM's metabolites and its residues of the active site, respectively [43]. The significance of these kinds of interactions lies in the fact that they are the primary directors of specificity, rate control, and reversibility in many biochemical reactions. Furthermore, it represents a first step in understanding oxidative damage in the active site produced by the TAM's metabolites and leads to identify their functioning and biological activity. Some authors use charge transfer to describe the oxidative damage of DNA bases [51, 52].

The interpretation of the value  $\Delta N$  is as follows: for  $\Delta N < 0$  the charge flows from A to B (A acts as an electron donor). For  $\Delta N > 0$  the charge flows from B to A (A acts as an electron acceptor). Therefore, in the presence of Glu353-Leu354, Leu349-Ala350-Asp351, and His524 residues,  $\Delta N$  of 4OHTAM accepts electrons, while for the rest of the residues it acts as an electron donor. END is an electron acceptor in the presence of the Trp383-Leu384 residue and with the remainder of the residues it acts as an electron donor. Finally, NDTAM acts as an electron acceptor in the presence of Glu353 and Leu349-Ala350-Asp351 residues, and as an electron donor with the remainder of the residues. The values are shown in **Table 3**.

The charge transfer descriptor is one of the noncovalent interactions that are present in biological systems in a macromolecule–ligand complex. In this case, the highest charge transfer value is in the same residue, Leu346-Thr347, for all the metabolites, which acts as a donor with amounts of  $-0.080$ ,  $-0.086$ , and  $-0.073$  for 4OHTAM, END, and NDTAM, respectively. Therefore, oxidative damage in the active site decreases in the order 4OHTAM > NDTAM > END.

Metabolite	Residue	$\Delta N$
4OHTAM	Gly521	-0.022
	Met388	0.089
	His524	0.004
	Lys529	-0.058
	Phe404	-0.010
	Trp383-Leu384	-0.012
	Glu353-Leu354	0.022
	Leu346-Thr347	-0.080
	Leu349-Ala350-Asp351	0.009
NDTAM	Gly521	-0.016
	Phe404	-0.004
	Glu353	0.047
	Leu428	-0.026
	His524-Lue525	-0.004
	Trp383-Leu384	-0.005
	Leu346-Thr347	-0.073
	Leu349-Ala350-Asp351	0.015
END	Gly521	-0.029
	His524	-0.004
	Leu387-Met388	-0.010
	Leu346-Thr347	-0.086
	Trp383-Leu384	0.001

**Table 3.** Charge transfer descriptor in the estrogen receptor.

### 3.2.5. Electrostatics interactions

Other noncovalent interactions between the ligand and hormone receptor are the hydrogen bond and  $\pi$ - $\pi$  interactions. An analysis of these bonds between the ER and each of TAM's metabolites was done. The results are as follows.

**4OHTAM.** This residue has one hydrogen bond (C=O----O-H) between the donor group (O-H) and the acceptor group (C=O) of the Gly521 residue. Also, there is a  $\pi$ - $\pi$  interaction between residue Trp383 and the planar core of the ligand.

**END.** There are two hydrogen bonds: first (C=O----OH) between the acceptor group (C=O) of Gly521 and the donor group (O-H) belonging to one of the rings and second (C=O----HN) between the accepting group (C=O) of Asp351 and the secondary amine (NH). The  $\pi$ - $\pi$  interaction was found among residue Trp383 and the planar core of the ligand.

*NDTAM*. In this metabolite was found one hydrogen bond (C=O---HN) between the accepting group (C=O) of Asp351 and the amine group of the ligand. No  $\pi$ - $\pi$  interactions were found in this ligand-receptor complex.

In all cases the metabolites analyzed followed the Lipinski et al. rule of five, which states: when there are five or fewer hydrogen bonds the drug will not present poor absorption or permeation and will be more active [53]. **Figure 4** shows the metabolites as a ball and stick and the residues of the active site as a tube. The hydrogen bonds are shown as green dots and  $\pi$ - $\pi$  interactions are the areas marked in yellow.

### 3.3. Analysis of the progesterone receptor with the metabolites

Analysis of molecular docking between PR and the metabolites is characterized by the active site of PR: the active site was described and the calculation and analysis of chemical reactivity

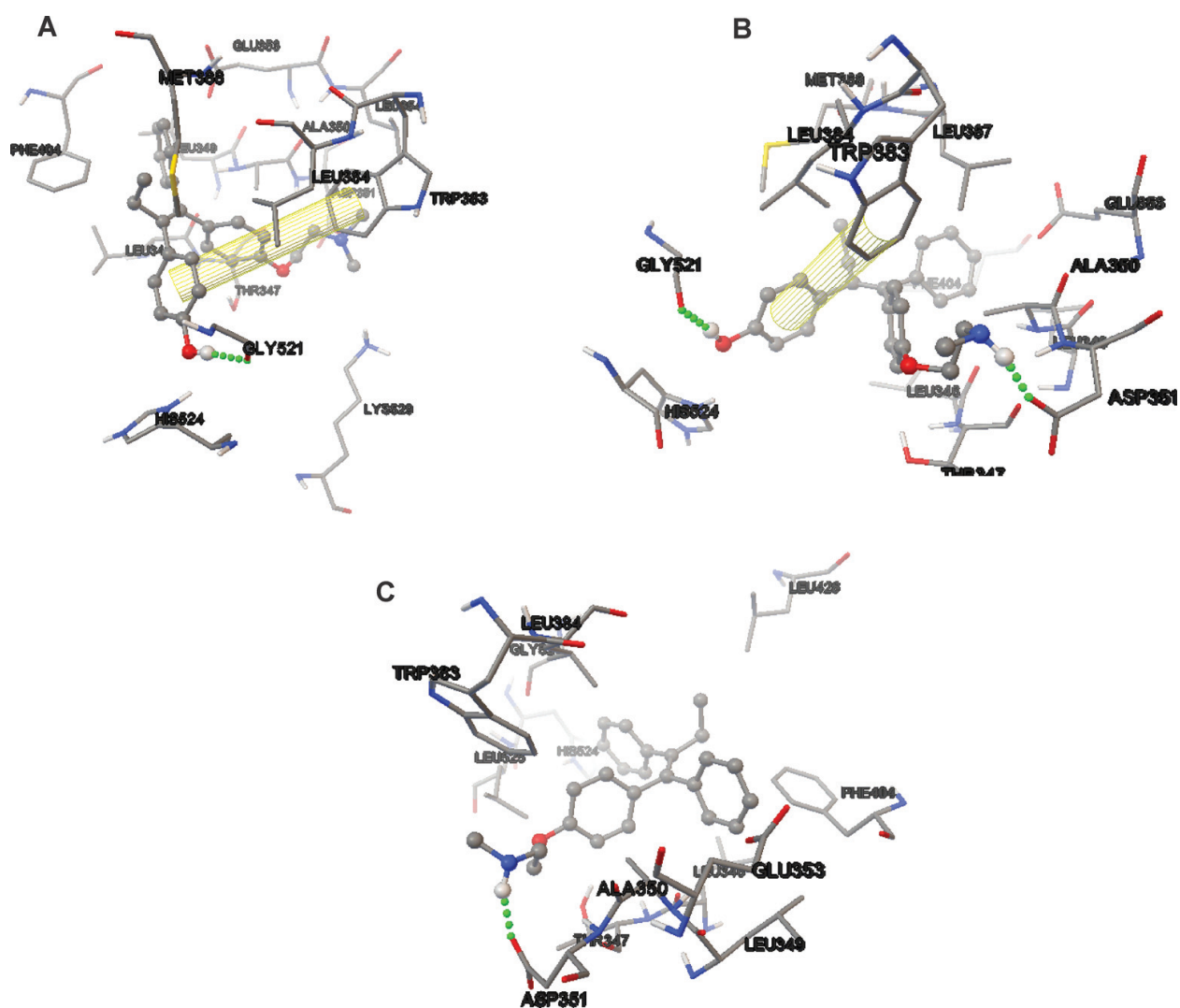


**Figure 4.** Hydrogen bond (green) and  $\pi$ - $\pi$  interactions (yellow) at the active site of the estrogen receptor with (A) 4OHTAM, (B) END, and (C) NDTAM.

parameters of the residues and metabolites were carried out, as well as the description of the hydrogen bond formed between the metabolites and the PR active site.

### 3.3.1. Molecular docking

The binding energy of TAM's metabolites at the active site of PR has been predicted by carrying out molecular docking calculations. The schematic structure of the active site and the binding energies are shown in **Figure 5**. The negative value of the binding energy in the

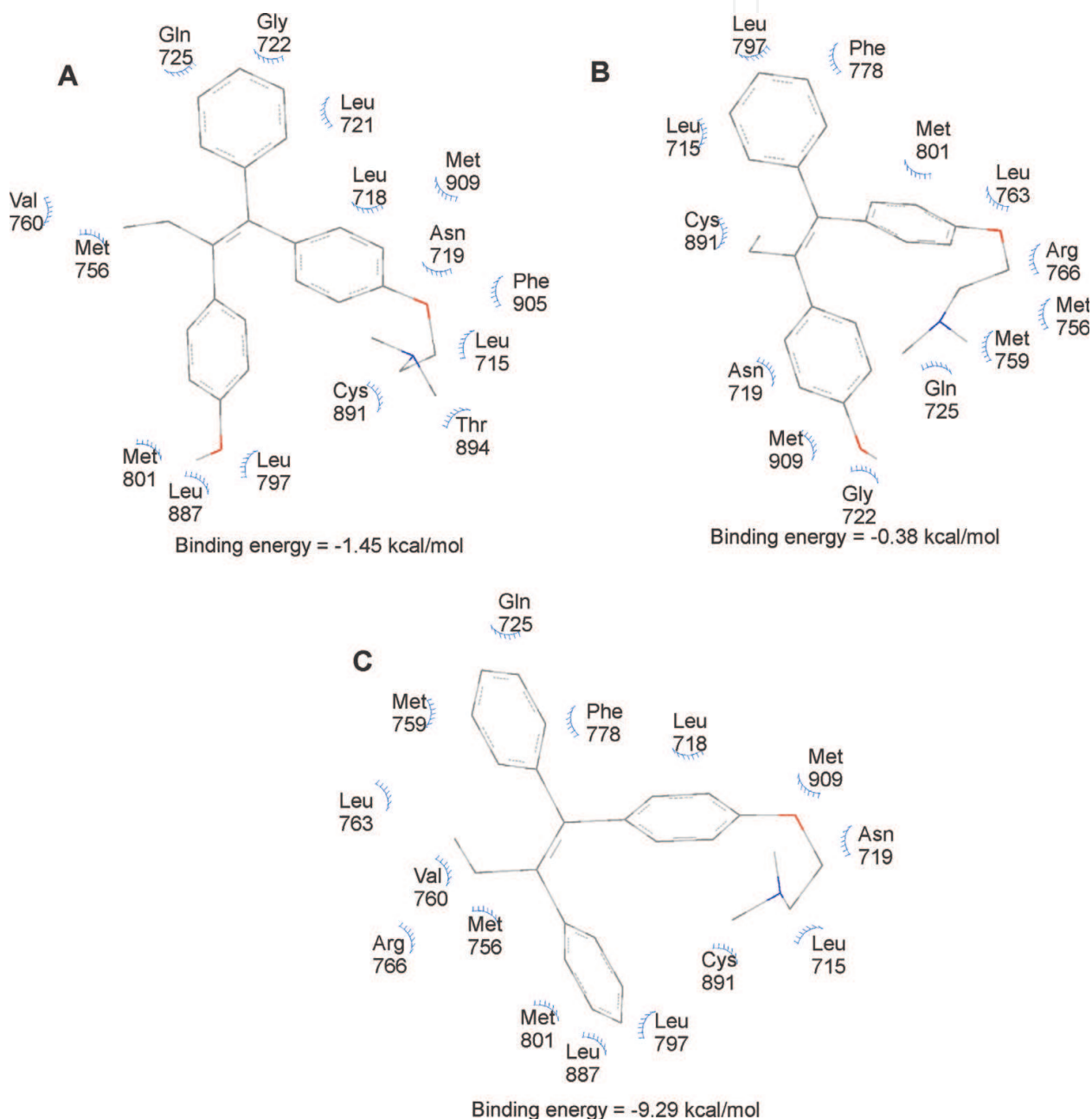


**Figure 5.** Amino acids of the active site of the progesterone receptor with (A) 4OHTAM, (B) END, and (C) NDTAM.

docking indicates that the system is stable and that there is an interaction between PR and metabolites at the site:  $-1.45$  kcal/mol for 4OHTAM,  $-0.38$  kcal/mol for END, and  $-9.29$  kcal/mol for NDTAM.

Although the metabolites END and 4OHTAM have a negative bond energy, their values remain very low compared to TAM, which has  $-9.38$  kcal/mol [13]. Therefore, these two metabolites will have very low biological activity in PRs.

### 3.3.2. Active site

The active site of PR obtained by theoretical analysis is as follows.

**4OHTAM.** There are 15 residues in contact with the metabolite 4OHTAM at the active site of PR. Four of them are linked, forming an amino acids sequence, leucine718-aspartic acid719 (Leu718-Asn719) and leucine721-glycine722 (Leu721-Gly722). The other 11 residues are highly hydrophilic: glutamine725 residue (Gln725), cysteine891 (Cys891), threonine894 (Thr894), and phenylalanine905 (Phe905); and seven are hydrophobic residues: methionine756, methionine801, and methionine909 (Met756, Met801, and Met909), valine760 (Val760), and leucine715, leucine797, and leucine887 (Leu715, Leu797, and Leu887).

**END.** The active site in END is formed by the following residues: glutamine725 (Gln725), cysteine891 (Cys891), glycine722 (Gly722), asparagine719 (Asn19), and arginine766 (Arg766), which are hydrophilic. The hydrophobic residues are phenylalanine778 (Phe778), tryptophan755 (Trp755), methionine756, methionine759, methionine801, and methionine909 (Met756, Met759, Met801, and Met909), and leucine715, leucine763, and leucine797 (Leu715, Leu763, and Leu797).

**NDTAM.** The active site for NDTAM consists of the following residues: leucine718-aspartic acid719 (Leu718-Asn 719) and methionine759-valine760 (Met759-Val760). Hydrophilic residues are glutamine725 (Gln725), arginine766 (Arg766), and cysteine891 (Cys891). Hydrophobic residues are phenylalanine778 (Phe778), methionine756, methionine801, and methionine909 (Met756, Met801, and Met909), and leucine715, lucine763, leucine797, and leucine887 (Leu715, Leu763, Leu797, and Leu887).

Most of the residues of the active site of 4OHTAM and END surround the planar core of the ligand and over the functional group amine. The steric hindrance of this amine group produces minor binding energy.

When the metabolites bind, there is a conformational change and they are recognized by the amino acids of the active site. This has to do with the coupling energies. In PR, NDTAM has a higher amount of binding energy exceeding  $-9$  kcal/mol.

Even when PR is more labile than ER, the binding energies indicate that the receptor is not sufficiently labile to recognize the metabolites 4OHTAM and END, which present binding energies lower than  $-1.5$  kcal/mol.

The residues for the metabolites in PR are shown in **Figure 5**.

### 3.3.3. Chemical reactivity

As soon as the most stable structure of the active site of TAM's metabolites was obtained, an analysis of the chemical reactivity of progesterone residues was performed by means of the reactivity descriptors. Results for these calculations are shown in **Table 4**.

Metabolite	Active site	EA (eV)	I (eV)	$\eta$ (eV)	$\mu = -\chi$ (eV)	$\omega$ (eV)
4OHTAM	Phe905	0.93	6.58	2.82	3.76	2.50
	Leu797	0.67	6.86	3.09	3.74	2.36
	Leu887	0.43	7.01	3.29	3.72	2.10
	Thr894	0.49	6.57	3.04	3.53	2.05
	Val760	0.76	6.92	3.08	3.84	2.40
	Met756	0.75	6.3	2.77	3.52	2.54
	Leu715	0.60	7.02	3.21	3.81	2.26
	Gln725	0.70	7.10	3.20	3.90	2.38
	Cys891	0.55	6.89	3.17	3.72	2.18
	Met801	0.64	6.27	2.82	3.45	2.12
	Met909	0.50	6.21	2.85	3.36	1.97
	Leu721-Gly722	-0.33	7.13	3.73	3.40	1.55
	Leu718-Asn719	1.06	7.06	3.00	4.06	2.74
	END	Arg766	0.21	7.03	3.41	3.62
Leu763		0.43	6.2	2.89	3.31	1.90
Gly722		0.51	6.25	2.87	3.38	1.99
Met759		0.88	7.74	3.43	4.31	2.71
Gln725		0.70	7.10	3.20	3.90	2.38
Trp755		0.86	5.85	2.50	3.35	2.25
Asn719		0.76	7.16	3.20	3.96	2.45
Leu797		0.67	6.86	3.09	3.74	2.36
Met756		0.75	6.30	2.77	3.52	2.54
Phe778		0.86	6.60	2.87	3.73	2.42
Leu715		0.60	7.02	3.21	3.81	2.26
Cys891		0.55	6.89	3.17	3.72	2.18
Met801		0.64	6.27	2.82	3.45	2.12
Met909		0.73	5.79	2.85	3.26	2.10
NDTAM	Leu763	0.35	7.17	3.41	3.76	2.07
	Leu797	0.67	6.86	3.09	3.74	2.36
	Leu887	0.43	7.01	3.29	3.72	2.10



Metabolite	Active site	EA (eV)	I (eV)	$\eta$ (eV)	$\mu = -\chi$ (eV)	$\omega$ (eV)
	Phe778	0.86	6.6	2.87	3.73	2.42
	Leu715	0.60	7.02	3.21	3.81	2.26
	Arg766	0.78	6.70	2.96	3.74	2.36
	Gln725	0.70	7.10	3.20	3.90	2.38
	Cys891	0.55	6.89	3.17	3.72	2.18
	Met756	0.75	6.30	2.77	3.53	2.24
	Met801	0.64	6.27	2.82	3.45	2.12
	Met909	0.50	6.21	2.85	3.36	1.97
	Met759-Val760	1.05	6.26	2.61	3.65	2.56
	Leu718-Asn719	1.06	7.06	3	4.06	2.74

**Table 4.** Parameters of chemical reactivity of the active site residues of the progesterone receptor.

The electron affinities of the residues fluctuate from  $-0.33$  eV to  $1.06$  eV. The highest value of electron affinity is for the Leu718-Asn719 residue, which is present in the active site of 4OHTAM, NDTAM, and the Met759 residue of END. The ionization potential results show that the greatest possibility of losing electrons is: Leu721-Gly722 with  $7.13$  eV in 4OHTAM, Leu763 with  $7.17$  eV in NDTAM, and Met759 with  $7.74$  eV in END.

Chemical hardness, the parameter that measures the resistance to change in the electronic configuration, exhibited amounts from  $2.50$  eV to  $3.73$  eV. In 4OHTAM, the lowest value and therefore the one that will react more easily in the presence of the metabolites is  $2.77$  eV for Met756. For END it is  $2.50$  eV in Trp755 and  $2.61$  eV in Met759-Val760. Met801 had a value of  $2.82$  eV in the NDTAM metabolite.

According to chemical potential, Met759 residue at  $-4.31$  eV presents the highest value in END. The electronegativity ( $\mu = -\chi$ ) shows that the Met759 residue has the greatest tendency to attract electrons at  $4.31$  eV in END. Electrophilicity  $\omega$  is the measure of the stabilization energy when systems become saturated by electrons from the surroundings. In this case in the active site of 4OHTAM value decreases in the following order: Leu718-Asn719 > Met756 > Phe905 > Val760 > Gln725 > Leu797 > Leu715 > Cys891 > Met801 > Leu887 > Thr894 > Met909 > Leu721-Gly722. In END the decreasing order is Met759 > Met756 > Asn719 > Phe778 > Gln725 > Leu797 > Leu715 > Trp755 > Cys891 > Met801 > Met909 > Gly722 > Arg766 > Leu763 and in NDTAM the decreasing order is Leu718-Asn719 > Met759-Val760 > Phe778 > Gln725 > Leu797 > Arg766 > Leu715 > Met756 > Cys891 > Met801 > Leu887 > Leu763 > Met909.

### 3.3.4. Charge transfer descriptor

Considering the high importance of this parameter in the formation of complexes in biological systems, the highest values in the different metabolites were defined. The charge transfer between metabolites and PR residues was calculated using Eq. 5. The results show that Met909 in 4OHTAM, Met909 and Leu763 in END, and Met909, Met756, Arg766, and Leu763

in NDTAM act as donor acceptors, namely, these residues are oxidized in the presence of the metabolites. The remainder of the residues act as electron acceptors. The values are shown in **Table 5**.

For 4OHTAM and NDTAM the maxima values are in Leu718-Asn719 with  $-0.064$  and  $-0.057$ , respectively. For END the maxima value is in Met759 with  $-0.088$ . Thus, the calculations

Metabolite	Residue	$\Delta N$	
4OHTAM	Leu718-Asn719	$-0.064$	
	Leu721-Gly722	$-0.002$	
	Phe905	$-0.037$	
	Leu797	$-0.033$	
	Leu887	$-0.03$	
	Thr894	$-0.014$	
	Val760	$-0.043$	
	Met756	$-0.014$	
	Leu715	$-0.039$	
	Gln725	$-0.047$	
	Cys891	$-0.031$	
	Met801	$-0.007$	
	Met909	$0.002$	
	END	Arg766	$-0.027$
		Leu763	$0.001$
		Gly722	$-0.006$
		Met759	$-0.088$
Trp755		$-0.003$	
Asn719		$-0.06$	
Leu797		$-0.04$	
Met756		$-0.020$	
Gln725		$-0.058$	
Phe778		$-0.041$	
Leu715		$-0.046$	
Cys891		$-0.037$	
Met801		$-0.013$	
Met909	$0.006$		
NDTAM	Leu763	$0.615$	
	Leu797	$-0.027$	
	Leu887	$-0.024$	
	Phe778	$-0.027$	

Metabolite	Residue	$\Delta N$
	Leu715	-0.033
	Arg766	0.665
	Gln725	-0.041
	Cys891	-0.025
	Met756	0.669
	Met801	-0.001
	Met909	0.008
	Met759-Val760	-0.021
	Leu718-Asn719	-0.057

**Table 5.** Transfer of charge between metabolites and progesterone receptor residues.

indicate that oxidative damage in the active site decreases in the following order: NDTAM > END > 4OHTAM.

### 3.3.5. Electrostatics interactions

An analysis of the hydrogen bond and  $\pi$ - $\pi$  interactions between the active site on PR and TAM's metabolites was performed. In the case of 4OHTAM and END metabolites no hydrogen bonds were generated, nor were there any  $\pi$ - $\pi$  interactions, whereas with NDTAM only a

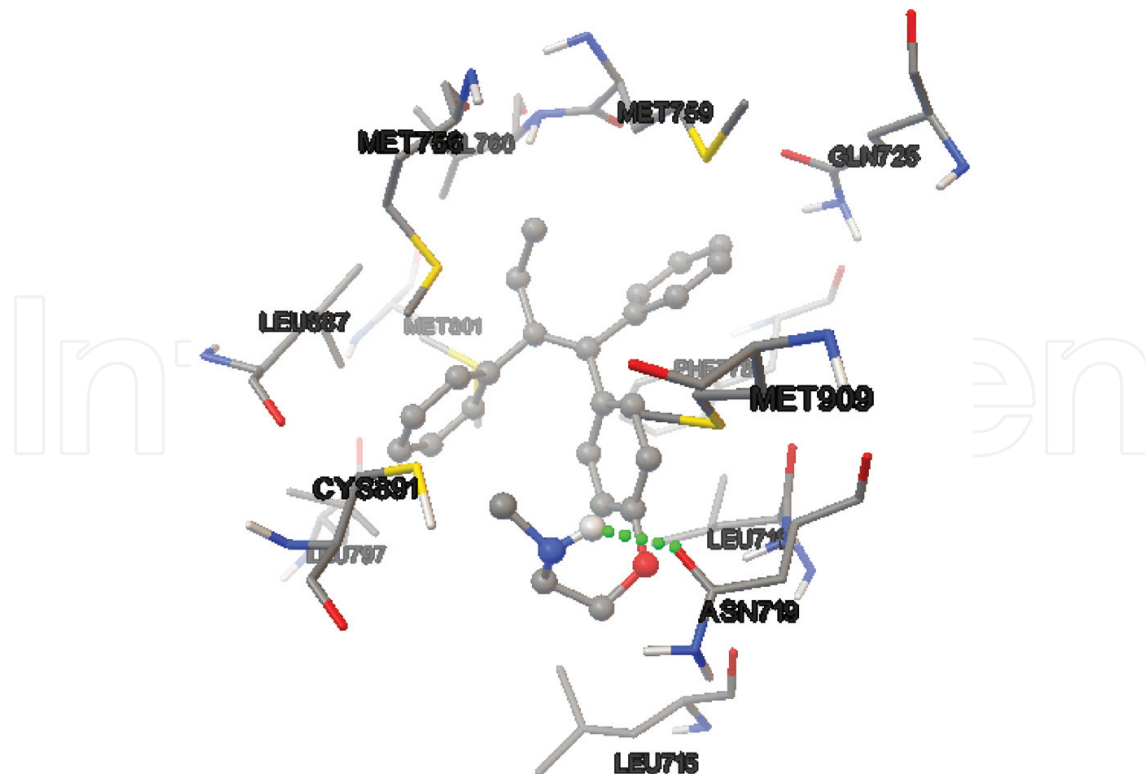


**Figure 6.** Hydrogen bond (green) at the active site of the progesterone receptor with the NDTAM metabolite.

hydrogen bond (C=O---H-N) was formed between the Asn719 residue and the amino group. The unique electrostatic interaction is shown with green dots in **Figure 6**. Also, it was found that the rule of five by Lipinski et al. [52, 53] was fulfilled.

#### 4. Conclusions

In this chapter the molecular docking of ER and PR with TAM's metabolites, 4OHTAM, NDTAM, and NDTAM, was analyzed. The amino acids sequence of the active site for each ligand-macromolecule complex was examined. The residues that constituted each active site were analyzed separately to find the charge transfer parameter, the hydrogen bond, and the  $\pi$ - $\pi$  interaction between the ligand and the receptor.

According to the binding energy obtained from docking, ER has greater stability than PR with the metabolites analyzed. However, in both cases there is a coupling between the receptor and the ligand, even when two of the binding energies in PR-ligand coupling are very small.

This coupling plays an important part in avoiding the transcription factor cascade reported by Leehy et al. [54].

This information agrees with the results of the chemical reactivity parameters, where it was found that the average of the chemical hardness values are lowest in active site residues of ER than in PR.

The charge transfer descriptor shows that TAM's metabolites mostly act as electron acceptors in their interaction with the hormone receptors. The hydrogen bonds in ER with END agree with the highest binding energy of this ligand. There are two hydrogen bonds, one  $\pi$ - $\pi$  interaction, and a  $\Delta N$  of  $-0.086$ . While in PR, there is only one hydrogen bond with NDTAM and the value of  $\Delta N$  is  $-0.057$ .

This work described the successful combination of the methods of molecular mechanics and electronic structure. It also explored the different conformational spaces and binding modes that allow smaller systems to work with them at the electronic level.

In addition to the above a significant conclusion is that the molecular modeling and simulations are an important improvement tool for any laboratory in many industries. Currently, many sectors are moving toward using more modeling and simulations in their laboratories. As Bernard Charlès, Dassault Systèmes CEO, states: "digitalization will mean big changes for everyday lab activities down the road." Two key solutions for all industries (such as pharmaceutical, chemical, life sciences, energy, and consumer goods) are collaboration and the ability to predict using simulation and modeling [55].

Patrick Bultinck et al. in their preface to the book *Computational Medicinal Chemistry for Drug Discovery* [21] wrote: "Nowadays, one can safely state that the computational chemist has become a respectable member of a drug design team." And we can add that the docking tool is essential for most techniques for structure-based drug design.

## Author details

Linda-Lucila Landeros-Martinez, Daniel Glossman-Mitnik, Erasmo Orrantia-Borunda and Norma Flores-Holguin\*

\*Address all correspondence to: norma.flores@cimav.edu.mx

NANOCOSMOS Virtual Lab, Department of Environment and Energy, Advanced Materials Research Center (CIMAV), Miguel de Cervantes 120, Complejo Industrial Chihuahua, Chihuahua, México

## References

- [1] Weidner N, Cady B, Goodson 3rd W. Pathologic prognostic factors for patients with breast carcinoma. Which factors are important. *Surgical Oncology Clinics of North America*. 1997;**6**(3):415-462
- [2] Veronesi U, Paganelli G, Galimberti V, Viale G, Zurrida S, Bedoni M, et al. Sentinel-node biopsy to avoid axillary dissection in breast cancer with clinically negative lymph-nodes. *The Lancet*. 1997;**349**(9069):1864-1867
- [3] Singletary SE, Allred C, Ashley P, Bassett LW, Berry D, Bland KI, et al. Revision of the American Joint Committee on Cancer staging system for breast cancer. *Journal of Clinical Oncology*. 2002;**20**(17):3628-3636
- [4] Molina M, Reigosa A, Nobrega D, Molina Y. Receptores de estrógeno y progesterona en cáncer de mama. Asociación con variables clinicopatológicas. *Revista Salus Online Facultad de Ciencias de la Salud Universidad de Carabobo (Valencia-Venezuela)*. 2001;**5**:34-42
- [5] Lai A, Kahraman M, Govek S, Nagasawa J, Bonnefous C, Julien J, et al. Identification of GDC-0810 (ARN-810), an orally bioavailable selective estrogen receptor degrader (SERD) that demonstrates robust activity in tamoxifen-resistant breast cancer xenografts. *Journal of Medicinal Chemistry*. 2015;**58**(12):4888-4904
- [6] Wardell SE, Nelson ER, Chao CA, Alley HM, McDonnell DP. Evaluation of the pharmacological activities of RAD1901, a selective estrogen receptor degrader. *Endocrine-related Cancer*. 2015;**22**(5):713-724
- [7] Srinivasan S, Nwachukwu JC, Bruno NE, Dharmarajan V, Goswami D, Kastrati I, et al. Full antagonism of the estrogen receptor without a prototypical ligand side chain. *Nature Chemical Biology*. 2016;**13**:111
- [8] Min J, Guillen VS, Sharma A, Zhao Y, Ziegler Y, Gong P, et al. Adamantyl antiestrogens with novel side chains reveal a spectrum of activities in suppressing estrogen receptor mediated activities in breast cancer cells. *Journal of Medicinal Chemistry*. 2017;**60**(14):6321-6336

- [9] Papageorgiou L, Cuong NT, Vlachakis D. Antibodies as stratagems against cancer. *Molecular BioSystems*. 2016;**12**(7):2047-2055
- [10] Altmeyer C, Karam TK, Khalil NM, Mainardes RM. Tamoxifen-loaded poly(L-lactide) nanoparticles: development, characterization and in vitro evaluation of cytotoxicity. *Materials Science and Engineering: C*. 2016;**60**:135-142
- [11] Khan MM, Wakade C, de Sevilla L, Brann DW. Selective estrogen receptor modulators (SERMs) enhance neurogenesis and spine density following focal cerebral ischemia. *Journal of Steroid Biochemistry and Molecular Biology*. 2015;**146**:38-47
- [12] Gao L, Tu Y, Wegman P, Wingren S, Eriksson LA. Conformational enantiomerization and estrogen receptor  $\alpha$  binding of anti-cancer drug tamoxifen and its derivatives. *Journal of Chemical Information and Modeling*. 2011;**51**(2):306-314
- [13] Irrarázaval OME. Tamoxifeno y antidepresivos: ¿Antagonistas en la prevención del cáncer de mama? *Revista médica de Chile*. 2011;**139**:89-99
- [14] Sanyakamdhorn S, Agudelo D, Bekale L, Tajmir-Riahi HA. Targeted conjugation of breast anticancer drug tamoxifen and its metabolites with synthetic polymers. *Colloids and Surfaces B: Biointerfaces*. 2016;**145**:55-63
- [15] Johnson MD, Zuo H, Lee K-H, Trebley JP, Rae JM, Weatherman RV, et al. Pharmacological characterization of 4-hydroxy-N-desmethyl tamoxifen, a novel active metabolite of tamoxifen. *Breast Cancer Research and Treatment*. 2004;**85**(2):151-159
- [16] Beverage JN, Sissung TM, Sion AM, Danesi R, Figg WD. CYP2D6 polymorphisms and the impact on tamoxifen therapy. *Journal of Pharmaceutical Sciences*. 2007;**96**(9):2224-2231
- [17] Ng HL. Simulations reveal increased fluctuations in estrogen receptor- $\alpha$  conformation upon antagonist binding. *Journal of Molecular Graphics and Modelling*. 2016;**69**:72-77
- [18] Landeros-Martínez LL, Orrantia-Borund E, Flores-Holguín N. Predicción de la reactividad química de Tamoxifeno en receptores hormonales. *Memorias Congreso de Investigación Científica Multidisciplinaria*. 2016;**4**(1):24-38
- [19] Kumar V, Jain G, Kishor S, Ramaniah LM. Chemical reactivity analysis of some alkylating drug molecules—a density functional theory approach. *Computational and Theoretical Chemistry*. 2011;**968**(1):18-25
- [20] Trott O, Olson AJ. AutoDock Vina: improving the speed and accuracy of docking with a new scoring function, efficient optimization, and multithreading. *Journal of Computational Chemistry*. 2010;**31**(2):455-461
- [21] Bultinck P, De Winter H, Langenaeker W, Tollenare JP. *Computational Medicinal Chemistry for Drug Discovery*. CRC Press; 2003
- [22] Mohan V, Gibbs AC, Cummings MD, Jaeger EP, DesJarlais RL. Docking: successes and challenges. *Current Pharmaceutical Design*. 2005;**11**(3):323-333

- [23] Kitchen DB, Decornez H, Furr JR, Bajorath J. Docking and scoring in virtual screening for drug discovery: methods and applications. *Nature Reviews Drug Discovery*. 2004;**3**(11): 935-949
- [24] DeLisle RK, Yu S-J, Nair AC, Welsh WJ. Homology modeling of the estrogen receptor subtype  $\beta$  (ER- $\beta$ ) and calculation of ligand binding affinities. *Journal of Molecular Graphics and Modelling*. 2001;**20**(2):155-167
- [25] Manas NHA, Bakar FDA, Illias RM. Computational docking, molecular dynamics simulation and subsite structure analysis of a maltogenic amylase from *Bacillus lehensis* G1 provide insights into substrate and product specificity. *Journal of Molecular Graphics and Modelling*. 2016;**67**:1-13
- [26] Maldonado-Rojas W, Olivero-Verbel J, Marrero-Ponce Y. Computational fishing of new DNA methyltransferase inhibitors from natural products. *Journal of Molecular Graphics and Modelling*. 2015;**60**:43-54
- [27] Berman HM, Westbrook J, Feng Z, Gilliland G, Bhat TN, Weissig H, et al. The Protein Data Bank. *Nucleic Acids Research*. 2000;**28**(1):235-242
- [28] Norgan AP, Coffman PK, Kocher J-PA, Katzmann DJ, Sosa CP. Multilevel parallelization of AutoDock 4.2. *Journal of Cheminformatics*. 2011;**3**(1):1
- [29] Morris GM, Ruth H, Lindstrom W, Sanner MF, Belew RK, Goodsell DS, et al. Software news and updates AutoDock4 and AutoDockTools4: automated docking with selective receptor flexibility. *Journal of Computational Chemistry*. 2009;**30**(16):2785-2791
- [30] Huey R, Morris GM, Olson AJ, Goodsell DS. A semiempirical free energy force field with charge-based desolvation. *Journal of Computational Chemistry*. 2007;**28**(6):1145-1152
- [31] Morris GM, Goodsell DS, Halliday RS, Huey R, Hart WE, Belew RK, et al. Automated docking using a Lamarckian genetic algorithm and an empirical binding free energy function. *Journal of Computational Chemistry*. 1998;**19**(14):1639-1662
- [32] Zhao Y, Truhlar D. The M06 suite of density functionals for main group thermochemistry, thermochemical kinetics, noncovalent interactions, excited states, and transition elements: two new functionals and systematic testing of four M06-class functionals and 12 other functionals. *Theoretical Chemistry Accounts*. 2008;**120**(1-3):215-241
- [33] Zhao Y, Truhlar DG. Density functionals with broad applicability in chemistry. *Accounts of Chemical Research*. 2008;**41**(2):157-167
- [34] Rassolov VA, Ratner MA, Pople JA, Redfern PC, Curtiss LA. 6-31G\* basis set for third-row atoms. *Journal of Computational Chemistry*. 2001;**22**:976-984
- [35] Tomasi J, Persico M. Molecular interactions in solution: an overview of methods based on continuous distributions of the solvent. *Chemical Reviews*. 1994;**94**(7):2027-2094
- [36] Hohenberg P, Kohn W. Inhomogeneous electron gas. *Physical Review*. 1964;**136**:B864-B871

- [37] Kohn W, Sham LJ. Self-consistent equations including exchange and correlation effects. *Physical Review*. 1965;**140**(4A):A1133-A1138
- [38] Robert G, Parr YW. *Density-Functional Theory of Atoms and Molecules*. New York, NY, USA: Oxford University Press; 1989
- [39] Frisch MJT, Trucks GW, Schlegel HB, Scuseria GE, Robb MA, Cheeseman JR, Scalmani G, Barone V, Mennucci B, Petersson GA, et al. *Gaussian 09*; Gaussian, Inc.: Wallingford, CT, USA; 2009
- [40] Hirshfeld FL. Bonded-atom fragments for describing molecular charge densities. *Theoretica Chimica Acta*. 1977;**44**(2):129-138
- [41] Pearson RG. Absolute electronegativity and hardness correlated with molecular orbital theory. *Proceedings of the National Academy of Sciences of the United States of America*. 1986;**83**(22):8440-8441
- [42] Parr RG, von Szentpály L, Liu S. Electrophilicity index. *Journal of the American Chemical Society*. 1999;**121**(9):1922-1924
- [43] Padmanabhan J, Parthasarathi R, Subramanian V, Chattaraj P. Electrophilicity-based charge transfer descriptor. *Journal of Physical Chemistry A*. 2007;**111**(7):1358-1361
- [44] DeLano WL. *The PyMOL molecular graphics system*. DeLano Scientific; Palo Alto, CA, USA; 2002
- [45] Samanta PN, Das KK. Prediction of binding modes and affinities of 4-substituted-2,3,5,6-tetrafluorobenzenesulfonamide inhibitors to the carbonic anhydrase receptor by docking and ONIOM calculations. *Journal of Molecular Graphics and Modelling*. 2016;**63**:38-48
- [46] Clarke R, Liu MC, Bouker KB, Gu Z, Lee RY, Zhu Y, et al. Antiestrogen resistance in breast cancer and the role of estrogen receptor signaling. *Oncogene*. 2003;**22**(47):7316-7339
- [47] Thomas G. *Fundamentals of Medicinal Chemistry*. Weinheim, Germany; 2003
- [48] Shiau AK, Barstad D, Loria PM, Cheng L, Kushner PJ, Agard DA, et al. The structural basis of estrogen receptor/coactivator recognition and the antagonism of this interaction by tamoxifen. *Cell*. 1998;**95**(7):927-937
- [49] Dávila JT, Garrán ADT. Moduladores selectivos de los receptores estrogénicos (SERMs): bioquímica, farmacología y aplicación clínica en ginecología. *Ginecología y Obstetricia de México*. 2005;**73**(08):424-435
- [50] Hall JM, McDonnell DP. The estrogen receptor  $\beta$ -isoform (ER $\beta$ ) of the human estrogen receptor modulates ER $\alpha$  transcriptional activity and is a key regulator of the cellular response to estrogens and antiestrogens. *Endocrinology*. 1999;**140**(12):5566-5578
- [51] Wan C, Fiebig T, Schiemann O, Barton JK, Zewail AH. Femtosecond direct observation of charge transfer between bases in DNA. *Proceedings of the National Academy of Sciences*. 2000;**97**(26):14052-14055



- [52] Kanvah S, Schuster GB. The sacrificial role of easily oxidizable sites in the protection of DNA from damage. *Nucleic Acids Research*. 2005;**33**(16):5133-5138
- [53] Lipinski CA, Lombardo F, Dominy BW, Feeney PJ. Experimental and computational approaches to estimate solubility and permeability in drug discovery and development settings. *Advanced Drug Delivery Reviews*. 2001;**46**(1-3):3-26
- [54] Leehy KA, Truong TH, Mauro LJ, Lange CA. Progesterone receptors (PR) mediate STAT actions: PR and prolactin receptor signaling crosstalk in breast cancer models. *Journal of Steroid Biochemistry and Molecular Biology*. 2018;**176**:88-93
- [55] Tulsi BB. A new generation. *Lab Manager* 2016;**11**(1):1-100